Visualizing the mechanism that determines the critical current density in polycrystalline superconductors using time-dependent Ginzburg-Landau theory

George J. Carty and Damian P. Hampshire
Superconductivity Group, Department of Physics, Durham University, Durham DH1 3LE, United Kingdom
(Received 27 March 2008; published 1 May 2008)

In polycrystalline superconducting materials optimized for high critical current density (J_C) in high magnetic fields, the mechanism that determines J_C has long remained uncertain because of the complicated manner in which the fluxon-fluxon and fluxon-microstructure forces combine. In this work, the time-dependent Ginzburg-Landau equations are used to produce visualizations of fluxons at J_C that show the disorder in the pinned part of the flux-line lattice and the motion of those fluxons along grain boundaries that cause dissipation. Calculated values of J_C are consistent with experimental data.

DOI: 10.1103/PhysRevB.77.172501 PACS number(s): 74.70.−b, 74.25.Sv, 74.25.Qt

Polycrystalline intermetallic superconductors are the critical component in nearly all commercial magnets operating above 10 T, including high-field NMR magnets and the high-field magnets of the $10 billion ITER fusion reactor. The most important design parameter for magnets is the critical current density (J_C), which determines their size and, hence, cost. The origins of the forces that act on the fluxons in a superconductor to determine J_C have been understood for decades. However, the forces add together in a manner so complex that there is no reliable description of the flux-line lattice (FLL) at criticality or which fluxons move within the superconductor during dissipation. The lack of theoretical understanding is exemplified by the widespread use of both flux-shear models[1–4] and flux-pinning models.[4,5] In flux-shear models, some fluxons are strongly pinned so that dissipation first occurs when unpinned fluxons overcome the fluxon-fluxon forces and shear past the stationary ones. In flux-pinning models, the fluxon-fluxon forces are broadly ignored and dissipation occurs when the Lorentz force provided by the macroscopic current is sufficient to move the fluxons out of the pinning sites.

In contrast to the theoretical uncertainty, there is a far clearer consensus about the properties of optimized materials: the experimental values of J_C achieved in high magnetic fields are 2 or 3 orders of magnitude below the depairing current density (or theoretical limit) and the reduced volume pinning force ($F_P/F_{P,\max}$, where the volume pinning force $F_P=BJ_C$, B is the magnetic field, and $F_{P,\max}$ is the maximum pinning force at constant strain and temperature) is a universal function of the reduced magnetic field ($b=B/B_{c2}$, where B_{c2} is the upper critical field).[1] The form of the universal function depends on the microstructure that leads to the optimum J_C.[1,6] In A15 polycrystalline materials (Nb_3Sn and Nb_3Al) where grain boundaries provide the important microstructure, J_C can be approximated by the Kramer scaling law[1] given by

$$F_P \approx A\frac{B_{c2}^{5/2}}{\mu_0\kappa^2}\sqrt{\frac{2\pi}{\phi_0}}b^{1/2}(1-b)^2, \qquad (1)$$

where κ is the Ginzburg-Landau parameter and $A\sim 1/500$. The functional form has been confirmed in detailed measurements in which magnetic field, temperature, and strain[7,8] were changed. Although such detailed measurements are not yet available for other polycrystalline superconductors, similar field dependence has also been observed in different A15 materials[1,8] as well as magnesium diboride,[9] the Chevrel-phase materials,[10,11] $YBa_2Cu_3O_{7-\delta}$ thin films,[12] and some NbTi samples where the Ti precipitate ribbons have been removed.[13] The main contribution of Kramer's original theoretical work was to explain how the universal scaling of F_P, which had been well established experimentally at that time, could arise. However, the details of the theory are not reliable since Kramer used an incorrect FLL shear modulus (C_{66}), which when corrected gives the wrong field dependence[14] for J_C. For simplicity, he also considered a two-dimensional (2D) system and assumed that the fluxons that sheared past stationary (pinned) fluxons were in a perfectly ordered hexagonal FLL. Much of the subsequent work in the literature that attempts to explain the Kramer functional form uses the same assumptions Kramer used including behavior specific to three-dimensional (3D) systems, such as fluxon bending or flux cutting is ignored and the FLL retains its hexagonal symmetry (i.e., disorder is ignored). Until now, there has been no way to assess the validity of these assumptions or the associated reliability of any of the proposed models or their predictions. The time-dependent Ginzburg-Landau[15,16] (TDGL) results presented here describe the spatial distribution of the order parameter for the superelectrons (ψ) and the magnetic field penetrating the polycrystalline superconductor. The visualizations of moving fluxons show the disorder in the pinned part of the flux-line lattice and the motion of those fluxons that cause dissipation. They allow us to see reliably the nature of the mechanism that determines J_C in polycrystalline materials in high magnetic fields.

Previous TDGL computational work used forward-time algorithms to analyze surface barriers[17,18] and FLL structures in layered 3D superconductors.[19] More recently, an efficient semi-implicit numerical algorithm[20] has been successfully developed to calculate J_C in superconductors with point pinning[21] and coatings.[22] This work uses the TDGL equations together with results from the Usadel theory for considering normal and superconducting components with different resistivities.[22] It provides the first report of calculations of J_C in a complex technological material,

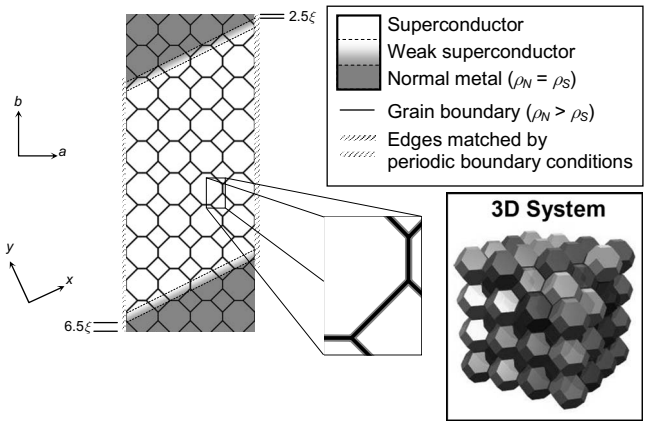

FIG. 1. Schematic of the simulated polycrystalline superconductor.

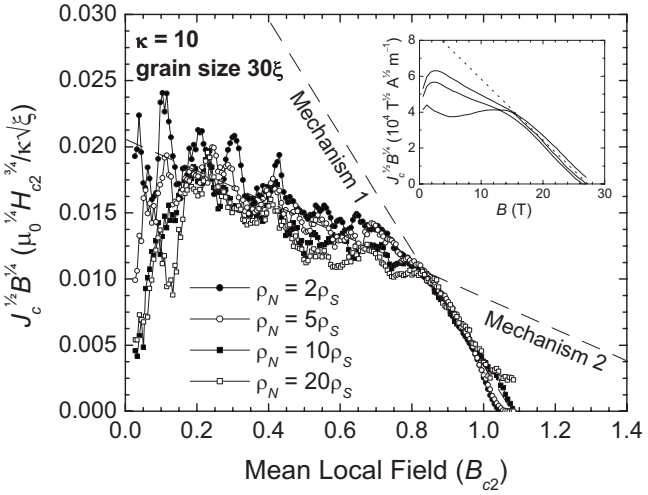

FIG. 2. Kramer plot for a 2D superconductor with $\kappa=10$, a grain size of 30ξ, $T=0.5T_C$, where the electric field E is given by $E \approx 10^{-8}H_{c2}\rho_S/\kappa^2\xi$ and $B_{c2}=\mu_0 H_{c2}$. Four values of the inner grain boundary resistivity ρ_N were considered. $2\rho_S$, $5\rho_S$, $10\rho_S$ and $20\rho_S$. The inset shows experimental data by Bonney (Ref. 28) for $SnMo_6S_8$. Two mechanisms are clearly discernible in both computational and experimental data.

namely, a bulk polycrystalline superconductor. The calculations were made practicable by using high-performance computers and this efficient algorithm,[20] which considers the entire grid rather than nearest neighbors only and gives about a factor of 1000 speed improvement[22] over conventional forward-time algorithms.

Figure 1 shows the layout of the simulated polycrystalline superconductor. The superconducting grains are identical truncated octahedra, which completely fill space. Cubic grains were considered undesirable because they would produce continuous planar boundaries that run through the entire material, which may have lead to artifacts not characteristic of real polycrystalline materials. All grain boundaries are of the same thickness. To remove macroscopic surface barrier effects, T_C is not reduced to zero instantaneously at the superconductor's edge, but over a distance of 10ξ, and a small fully normal region is included at the extrema.[22,23] The macroscopic edges of the superconductor are angled with respect to the grain boundary structure to smooth the local spatial variations in field,[24] thus reducing the uncertainty in J_C values. Both 2D and 3D calculations are presented in this work. For the 2D calculations, the x-y cross section chosen was as shown in Fig. 1.

The grain boundaries are simulated as normal-metal trilayers, with an inner layer of thickness ξ with increased resistivity and outer layers each of thickness ξ, where the resistivity is the same as the normal-state resistivity of the superconductor. Hence, the reduction in T_C occurs over a longer range than the range over which the resistivity increase occurs. This is consistent with T_C being more sensitive to strain[25] than the normal-state resistivity. This trilayer structure also ensured that superconductivity did not persist near the edges of the grains above the bulk value of B_{c2}—in agreement with experiments[26] that show similar B_{c2} values for polycrystalline materials and single crystals.

An external magnetic field was applied to the polycrystalline superconductor. Consistent with Bean's model, the fluxons arrange to produce macroscopic screening currents and an associated gradient in flux density.[27] J_C was then obtained by using a least-squares fit to the spatial gradient of the local field together with one of Maxwell's equations in a procedure analogous to a magnetization measurement.[27] Calculation of J_C as a function of field in polycrystalline superconductors is very computationally expensive even with the efficient algorithm. Therefore, a fast sweep from zero field to above B_{c2} and back to zero again was first used to provide initial conditions for the local magnetic field and order parameter. Then, at any required field, the initial conditions were established and the applied magnetic field was held constant so that the internal electric fields equilibrated toward zero and a value of J_C obtained. Since we are principally concerned with high-field J_C, the data are plotted in the form of Kramer plots.

Figure 2 shows J_C as a function of B for a 2D superconductor with $\kappa=10$ and a grain size of 30ξ across for grain boundaries with four different inner layer resistivities. The standard dimensionless units for TDGL computation have been used.[22,23] These data show that J_C is not significantly affected by changes in the inner grain boundary resistivity. Matching effects (oscillations) are observed in the low-field data that result from the periodicity of the grains structures. The distinct kink at about $0.8\ B_{c2}$ suggests that there is one mechanism operating in low fields and a different one in high fields. A similar two-mechanism field dependence is shown in the inset of Fig. 2, which is the experimental data on the Chevrel-phase material $SnMo_6S_8$,[28] and has also been observed by Kramer in the A15 Nb_3Sn.[29]

Other 2D computational data (not shown) demonstrate that the low-field properties are particularly complex since there is no simple functional form for J_C and, for example, J_C decreases for very small grains consistent with the normal volume fraction of the system increasing. This work focuses on the high-field mechanism where there is experimental consensus about Eq. (1), and in two dimensions, we have computationally confirmed that $J_C \propto 1/\kappa^2$ and is independent of grain size. The prefactor A is weakly width dependent, but for the data shown is 1.6×10^{-3}, which is within 20% of the

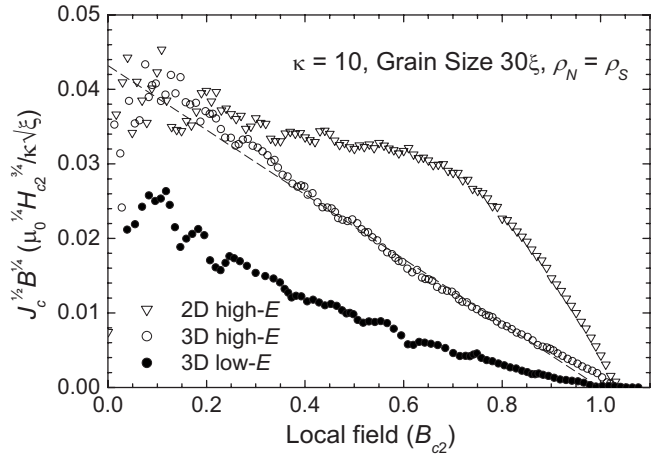

FIG. 3. Kramer plot comparing high E ($\approx 10^{-4} H_{c2} \rho_S / \kappa^2 \xi$) and low E ($\approx 10^{-8} H_{c2} \rho_S / \kappa^2 \xi$) J_C for 2D and 3D systems.

experimental values in Nb_3Sn,[8] and Nb_3Al.[30] Figure 3 compares J_C for equivalent 2D and 3D systems (an inner grain boundary resistivity $\rho_N = \rho_S$ was chosen to speed the computation, effectively giving monolayer grain boundaries). In three dimensions, the Kramer dependence of J_C extends to lower fields than that in two dimensions. Indeed, for the high E-field data, it extends over the entire field range—a field dependence observed experimentally.[14] The J_C values presented are not very sensitive to the E-field criterion at which they are calculated—J_C changes by about a factor of 4 when the E-field changes by 4 orders of magnitude. The $(1-b)^2$ factor in high-field J_C, which is observed in the 2D and 3D computational results, as well as in experimental data, points toward a flux-shear mechanism. A video of 2D computational data[32] with an applied transport current just above J_c shows distorted fluxons shearing along grain boundaries. The visualization identifies flux flow by highly distorted fluxons past (almost) stationary fluxons in the grains with almost no hexagonal symmetry as the mechanism that determines J_C in polycrystalline materials. Flux flow along grain boundaries past an ordered hexagonal FLL has been proposed before[2–4] but the visualization shows the following: the fluxons that move along grain boundaries are strongly distorted (i.e., not circular) particularly at the grain boundary triple points; the order parameter is strongly depressed along all the grain boundaries; there is a wide fluxon-free layer next to the grain boundaries along which a large current flows; the fluxons within the grains are almost stationary and their arrangement or order is strongly affected by the shape of the grains rather than having hexagonal symmetry. Hence, this work provides the means to identify the important characteristics or approximations that can be used to reliably explain the Kramer functional form. We have found in polycrystalline materials with much larger grain size and much lower J_C than considered here that the hexagonal symmetry does occur as expected in the interior of the grains. In high B fields, the prefactor A for 3D computational systems is about one-fifth of that for two dimensions. This result can be explained by a simple geometric argument since in the 3D system only about one-fifth of the flux lines confined to the grain boundaries are parallel to the applied field (and thus have their motion resisted by fluxon-fluxon interactions). This suggests that a 2D system contains most of the important physical processes operating in the 3D system. Figure 4 shows a snapshot of $|\psi|^2$ in selected x-y and y-z planes in a 3D superconductor. Fluxons in the grain interiors are predominantly parallel to the applied field, although they bend slightly toward the local normal to a grain boundary on entry or exit. Visualization of the normal current (and thus the dissipation) shows that in three dimensions, as in two dimensions, most of the dissipation is in or near the grain boundaries, implying that those sections of fluxons passing through grain interiors remain almost stationary when a current exceeding J_C is applied and the dissipation is due to fluxons that move along the grain boundaries.

The superconductors studied in this work have rather simplistic grain boundaries (no dislocations or complex compositional variations) but nevertheless lead to J_C values similar to experimental observations. The extended calculations presented here allow the reader to see a visualization of flux motion in polycrystalline superconductors derived using TDGL and, hence, reliably assess the validity and accuracy of the approximations and assumptions made that underpin

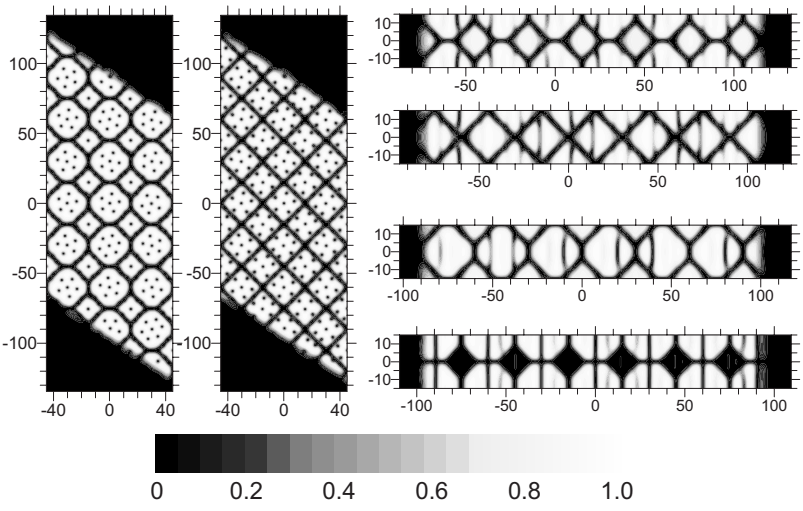

FIG. 4. Snapshots of the order parameter for the superelectrons squared ($|\psi|^2$) in x-y (at two different points along the z axis) and of y-z cross sections of a 3D polycrystalline superconductor with $\kappa = 10$ at $H = 0.151 H_{c2}$. The grain boundaries are equivalent to 2ξ-thick monolayers with $\rho_N = \rho_S$. The spatial axes are calibrated in units of the coherence length ξ.

the phenomenological models for J_C in the literature. Our preliminary investigations into the effect of changing the detailed properties of grain boundaries show that increases in J_C can, for example, be obtained by changing the effective B_{c2} of the superconductor by introducing high resistivity superconducting layers near the grain boundaries. One can also consider removing the grain boundaries altogether, as has been successful in developing high temperature superconductors with high J_C.[31] Computation similar to that presented here will enable us to more efficiently engineer superconducting materials with J_C properties closer to the theoretical limit.

[1] E. J. Kramer, J. Appl. Phys. **44**, 1360 (1973).
[2] A. Pruymboom, W. H. B. Hoondert, H. W. Zandbergen, and P. H. Kes, Jpn. J. Appl. Phys., Suppl. **26** 1529 (1987).
[3] A. Pruymboom, P. Kes, E. Drift, and S. Radelaar, Appl. Phys. Lett. **52**, 662 (1988).
[4] D. Dew-Hughes, Philos. Mag. B **55**, 459 (1987).
[5] D. Dew-Hughes, Philos. Mag. **30**, 293 (1974).
[6] R. Hampshire and M. Taylor, J. Phys. F: Met. Phys. **2**, 89 (1972).
[7] D. M. J. Taylor and D. P. Hampshire, Supercond. Sci. Technol. **18**, S241 (2005).
[8] S. A. Keys and D. P. Hampshire, Supercond. Sci. Technol. **16**, 1097 (2003).
[9] D. Larbalestier *et al.*, Nature (London) **410**, 186 (2001).
[10] N. Cheggour, M. Decroux, Ø. Fischer, and D. P. Hampshire, J. Appl. Phys. **84**, 2181 (1998).
[11] N. Cheggour, M. Deroux, A. Gupta, Ø. Fischer, J. A. A. J. Pederboom, V. Bouquet, M. Sergent, and R. Chevrel, J. Appl. Phys. **81**, 6277 (1997).
[12] M. Saleh, Y. A. Hamam, M. R. Said, M. Abu Samrah, and I. Abu Aljarayesh, Supercond. Sci. Technol. **13**, 1607 (2000).
[13] Y. Yamada, S. Murase, Y. Kamisada, E. Suzuki, H. Wada, and K. Tachikawa, Philos. Mag. B **52**, 23 (1985).
[14] D. P. Hampshire, H. Jones, and E. W. J. Mitchell, IEEE Trans. Magn. **21**, 289 (1985).
[15] A. Schmid, Phys. Kondens. Mater. **5**, 302 (1966).
[16] C.-R. Hu and R. S. Thompson, Phys. Rev. B **6**, 110 (1972).
[17] D. Y. Vodolazov, Phys. Rev. B **62**, 8691 (2000).
[18] M. Machida and H. Kaburaki, Phys. Rev. Lett. **71**, 3206 (1993).
[19] M. Machida and H. Kaburaki, Phys. Rev. Lett. **74**, 1434 (1995).
[20] T. Winiecki and C. S. Adams, J. Comput. Phys. **179**, 127 (2002).
[21] T. Winiecki and C. S. Adams, Phys. Rev. B **65**, 104517 (2002).
[22] G. J. Carty, M. Machida, and D. P. Hampshire, Phys. Rev. B **71**, 144507 (2005).
[23] J. E. Evetts, Phys. Rev. B **2**, 95 (1970).
[24] C. P. Bean, Phys. Rev. Lett. **8**, 250 (1962).
[25] J. W. Ekin, Cryogenics **20**, 611 (1980).
[26] J. P. Hurault, Phys. Lett. **20**, 587 (1966).
[27] C. P. Bean, Rev. Mod. Phys. **36**, 31 (1964).
[28] L. A. Bonney, T. C. Willis, and D. C. Larbalestier, J. Appl. Phys. **77**, 6377 (1995).
[29] E. J. Kramer, J. Electron. Mater. **4**, 839 (1975).
[30] S. A. Keys, N. Koizumi, and D. P. Hampshire, Supercond. Sci. Technol. **15**, 991 (2002).
[31] M. Tomita and M. Murakami, Nature (London) **421**, 517 (2003).
[32] http://www.dur.ac.uk/superconductivity.durham/fluxflow.html